

Role of Subsurface Layer Temperature Inversion in cyclone induced warming in the northern Bay of Bengal

**Anand P¹ Jimna Janardhanan CM² Anakha P Nair³ Suresh. I⁴ V. Suneel⁴ Gopika S⁴
Pankajakshan Thadathil³**

¹ Naval Physical and Oceanographic Laboratory

² Cochin University of Science and Technology

³ Kerala University of Fisheries and Ocean Sciences

⁴ National Institute of Oceanography

Corresponding author: Anand P, anandp.npol@gov.in

Abstract:

Subsurface Layer Temperature Inversion (SLTI) is a prominent physical process occurring in the Bay of Bengal (BoB) during winter. BoB also witnesses intense cyclones during winter (post-monsoon). Sidr is a category-5 cyclone that occurred in the BoB during 11-15 November 2007. The present study emphasises bringing out the effect of SLTI on SST warming. This paper uses observations and modelling to present SLTI's role in surface layer post-cyclone warming. In the absence of SLTI, the cyclone induces surface cooling. However, in the case of a surface layer with SLTI, instead of cooling, sea surface warming of <0.5 °C is observed near the head bay, where SLTI is prominent. Model results and observations suggest the role of entrainment and warming of the surface layer

Keywords: Tropical Cyclone, Subsurface Layer Temperature Inversion, entrainment, sea surface temperature variability

Highlights:

- Subsurface Layer Temperature Inversion (SLTI) is a significant large-scale process in the Bay of Bengal.
- This paper uses observations and modelling to present SLTI's role in surface layer post-cyclone warming.
- Model results and observations suggest the role of entrainment and warming of the surface layer.

Introduction

Tropical Cyclones (TC) majorly occur in the North Indian Ocean (NIO) during pre-monsoon (early April-June) and post-monsoon (October-December) seasons (Mondal et al., 2002). The number of occurrences is more during pre-monsoon than post-monsoon (Nadimpalli et al. 2021). The strong wind shear during the monsoon limits cyclone formation (Li et al., 2013). Though the percentage of cyclone occurrence is less in the Indian Ocean (6% of the global ocean), 80% of the global fatalities occur in this region (Ali 1999; Beal et al. 2020; Longshore 2008; Neetu et al. 2012).

TC forces the ocean surface by bringing subsurface cold water, cooling the surface layer. During pre-monsoon, the TC-induced surface cooling in the BoB varies from 2 to 3 °C (Rao, Joshi, and Ravichandran 2008; Krishna et al. 1993; Sengupta, Goddalahundi, and Anitha 2008) whereas, the post-monsoon cooling varies from 0.5 - 1 °C (Subrahmanyam et al. 2005; Sengupta, Goddalahundi, and Anitha 2008). Cyclone-induced cooling is generally observed more in the south BoB, and the cooling decreases towards the north (Pothapakula et al. 2017)

The reason for the observed lesser post-monsoon cooling is due to the existence of freshwater-induced salinity stratification in the northern BoB. As a result, during post-monsoon, a thick barrier layer (BL) occurs in the northern BoB (Thadathil et al., 2007; Webster et al., 2002; Vinayachandran, Murty, and Ramesh Babu, 2002). BL suppresses the entrainment of subsurface cold water to the surface and reduces surface cooling (Sprintall and Tomczak 1992). The existence of BL decreases TC-induced surface cooling and promotes cyclone intensification through positive feedback. Maneesha et al. (2012) reported the role of BL in reducing the surface cooling in the BoB and intensification of cyclone Nargis in April 2008.

Using both observations and model, Balaguru et al. (2012) demonstrated reduced surface cooling and TC intensification associated with the presence of BL in the tropical Atlantic, Indian and Pacific oceans. Using a model, Jullien et al. (2014) reported increased cyclone intensity in the South Pacific Ocean due to increased BL thickness. Sengupta, Goddalahundi and Anitha (2008) and Neetu et al. (2012) compared the pre-monsoon and post-monsoon TC-induced cooling in the BoB. They attributed the less cooling in the post-monsoon season to the presence of thick BL. Navaneeth et al. (2019) observed a weak SST cooling in the wake of cyclone Phailin due to strong near-surface haline stratification.

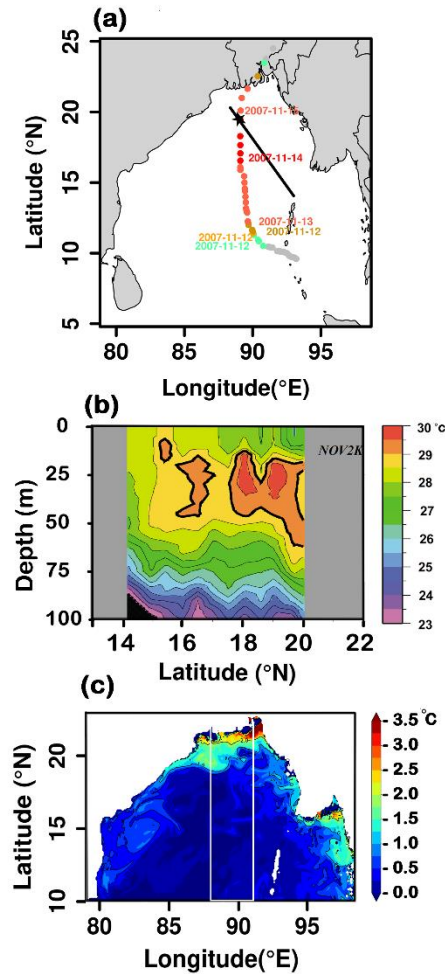


Figure 1: (a) Study region showing cyclone track (filled solid circles with colour shade ranging from light green(category-1) to dark red (category-5)) and TOGA-XBT line from Port Blair to Kolkata (solid black line). (b) Vertical section of temperature for November 2000 along the TOGA-XBT line. (c) Distribution of SLTI in the BoB for 9 November 2007 from GLORYS model. The rectangle in white line shows the TC induced SST anomaly area considered in figure-2a.

In the northern BoB, during post-monsoon, the BL is modified with SLTI, a warm layer sandwiched between a colder surface and a subsurface layer (Thadathil et al. 2002). Mathew et al. (2018) reported sea surface warming induced by the passage of cyclone Thane over the SLTI zone in the south-western BoB, even with a low ($\Delta t < 2$ °C) SLTI gradient. The southern BoB has significantly less SLTI than the head bay ($\Delta t \sim 5$ °C) (Thadathil et al. 2002). Therefore, the role of SLTI is examined in TC-induced warming in the prominent SLTI regions. For this purpose, in the present study, we consider a category-5 cyclone, Sidr, which occurs from 11-15 November 2007 and has a near longitudinal track to cross the SLTI intense zone near the head bay (Figure 1a). Vissa et al. (2013) highlight the observed less cooling after the passage of cyclone Sidr due to the presence of BL south of the region selected in the present study without considering the role of SLTI. This paper

uses observations and modelling to present SLTI's role in surface layer post-cyclone warming. Section-2 summarises the data and method used in this study. Section-3 illustrates the results obtained from the model and other observations, followed by a discussion in section-4.

Data and Method

Sidr, an extremely severe cyclone, occurred in BoB during 11-15 November 2007, causing one of the worst natural disasters in India and Bangladesh. It formed in the central BoB on 11 November 2007 and became a category-5 TC (Saffir–Simpson scale), eventually landfall in Bangladesh on 15 November. The cyclone parameters were obtained from the International Best Track Archive for Climate Stewardship (IBTrACS; Knapp et al. 2010) dataset. Filled solid circles represent the cyclone track (Figure 1a), with colour shades ranging from light green (category-1) to dark red (category-5).

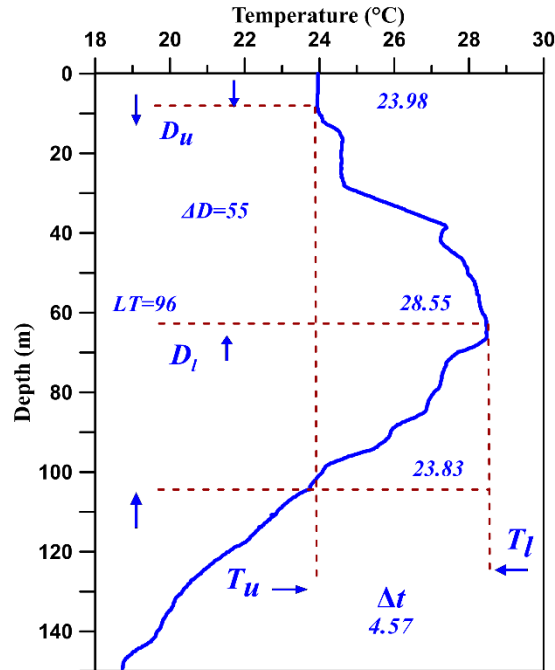


Figure 2: Schematic of the SLTI characteristics (D_u – Upper depth limit of Temperature Inversion; D_l – Lower depth limit of Temperature Inversion; T_u – Temperature at D_u , T_l – Temperature at D_l ; ΔD – Depth difference of D_l and D_u ; ΔT – Temperature difference between D_l and D_u ; LT – Inversion layer thickness)

The SLTI is noticed to have very high intra-seasonal variability in the NIO. The major causative factors for the SLTI are freshwater flux, surface heat flux, and surface advection (Thadathil et al. 2002, 2016). Detailed investigation of SLTI, its causative factors, characteristics, stability, inter-annual variability and generating mechanism, etc., has been done by many researchers (Thadathil et al. 2002, 2007, 2016; Vinayachandran, Murty, and Ramesh Babu 2002; Jian et al. 2012; Chowdhury

2022a, b). SLTI characteristics, such as the gradient of the inversion layer (Δt) and inversion layer thickness (LT), are illustrated in Figure 2. Considering the XBT temperature profile spikes and sensor accuracy, the Δt threshold is fixed at 0.5 °C and the LT threshold at 5 m (Thadathil et al. 2002). In the present study, we use the Global Ocean Reanalysis and Simulations (GLORYS) (Lellouche et al. 2018) and Princeton Ocean Model (POM model) (Blumberg and Mellor 1987) temperature data during November 2007 to understand the spatial and vertical structure of SLTI. The horizontal distribution of SLTI during November 2007 has been derived from GLORYS. Temperature data along 89.5°E (Matching the cyclone track) have been derived from GLORYS and POM. GLORYS v1 database (Lellouche et al. 2018) is produced under the framework of the European Copernicus Marine Environment Monitoring Service. GLORYS v1 is a global reanalysis product, available daily at an eddy-resolving 1/12° horizontal resolution and 50 standard vertical levels during the 1993-present day. GLORYS uses NEMO (Nucleus for European Modeling of the Ocean) as its model component and a reduced-order Kalman filter for assimilating sea level anomaly, temperature, and salinity observations, with a 3D-VAR scheme to reduce large-scale bias. The model is forced with European Centre for Medium-Range Weather Forecasts (ECMWF) ERA-Interim (Dee et al. 2011), and ERA5 reanalysis (Hersbach et al. 2020) atmospheric fluxes. GLORYS provides reliable assessments and accurate estimates of ocean features (Verezemskaya et al. 2021).

POM (Blumberg and Mellor 1987) with realistic bottom topography (Sindhu et al. 2007) also addresses the role of entrainment associated with Sidr. More details of the model for the Indian Ocean scenario are given in Rao, Joshi, and Ravichandran (2008) and Kumar et al. (2009). In this study, a multi-grid POM model with a fine resolution domain (80°-100°E, 10°-25°N) within the coarse resolution (38°E to 118°E and 14°S to 26°N) is employed. The model uses a time-splitting technique with 20 s and 400 s time intervals for barotropic and baroclinic modes, respectively. The open boundary condition is set as radiation condition. Initial temperature and salinity fields are obtained from the World Ocean Atlas 2018 (Garcia et al. 2019). The model is forced by wind, solar radiation and net heat flux data from ECMWF ERA5 fifth-generation reanalysis (Hersbach et al. 2020), and assimilation is done using Copernicus Marine Environment Monitoring Service (CMEMS) SLA data and ECMWF ERA5 reanalysis (Hersbach et al. 2020) SST data obtained from climate data store-Copernicus. A 20-year spin-up is performed for the model forced by climatology wind and heat flux to get a steady state. Subsequently, the model is forced from September 2007 to January 2008. TOGA-XBT data for 2000, 2006, 2007 and 2009 have been obtained from the National Institute of Oceanography, Goa, India.

In order to understand the possible role of entrainment in the observed sea surface warming after the

passage of cyclone, the mixed layer heat budget at the centre of the warming region is examined for pre-cyclone, cyclone and post-cyclone dates. The heat budget analysis of Rao and Sivakumar (2000) had used in this study.

$$\frac{\partial T}{\partial t} = \frac{Q_{net} - Q_{pen}}{\rho C_p h} - \left[u \frac{\partial T}{\partial x} + v \frac{\partial T}{\partial y} \right] + Residual$$

where $\frac{\partial T}{\partial t}$ is the mixed layer temperature tendency, the first term on the RHS represents the heat fluxes due to atmospheric forcing, in which Q_{net} is the net surface heat flux, Q_{pen} is the penetrative shortwave below the mixed layer, ρ (=1023 kg/m³) is the density of seawater, C_p (=3989.2 J/kg.K) is the specific heat capacity of seawater, and h is the MLD. The terms $-u \frac{\partial T}{\partial x}$ and $-v \frac{\partial T}{\partial y}$ are the zonal and meridional components of horizontal advection, respectively. The residual mainly accounts for the vertical processes (entrainment and vertical diffusion Surface latent heat flux (Q_{lat}), surface sensible heat flux (Q_{sen}), surface net solar radiation (Q_{short}) and surface net thermal radiation (Q_{long}) daily data are downloaded from ERA-interim at 12 noon at 0.125 x 0.125 spatial resolution for November 2007. (<https://apps.ecmwf.int/datasets/data/interim-full-daily/levtype=sfc/>). Temperature daily mean fields are used from GLORYS product ‘Global Ocean 1/12° Physics Analysis and Forecast updated Daily’ at 0.083°x0.083° which is interpolated to 0.125°x0.125° (https://data.marine.copernicus.eu/product/GLOBAL_ANALYSISFORECAST_PHY_001_024/services). Q_{pen} is estimated as,

$$Q_{pen} = 0.47 Q_{short} \left[V_1 e^{-\frac{h}{\zeta_1}} + V_2 e^{-\frac{h}{\zeta_2}} \right]$$

where ζ_1 is the attenuation depths of long visible and ζ_2 is the attenuation depths of short visible and ultraviolet wavelengths, and h is the MLD in meters [Morel and Antoine, 1994; Sweeney et al., 2005]. As in Girishkumar et al., [2013], the values of V_1 , V_2 , ζ_1 and ζ_2 are 0.39, 0.69, 1.52, and 18.9 respectively.

Results

During winter, the northern BoB witnesses large-scale SLTI with the inversion gradient reaching 5°C (Thadathil et al. 2002). This warmer layer just below a very shallow mixed layer is a potential heat source for the surface layer once it is tapped by entrainment by the passage of the cyclone. Figure 1b illustrates the XBT temperature section from Kolkata to Andaman during November 2000 along the TOGA-XBT track shown as solid black line in Figure 1a. The spatial distribution of the

SLTI on 11 November 2007 (GLORYS model) shows that the SLTI is more prominent towards the northern bay (Figure 1c) with a variability of 0 to 3.5°C from the southern to the northern bay.

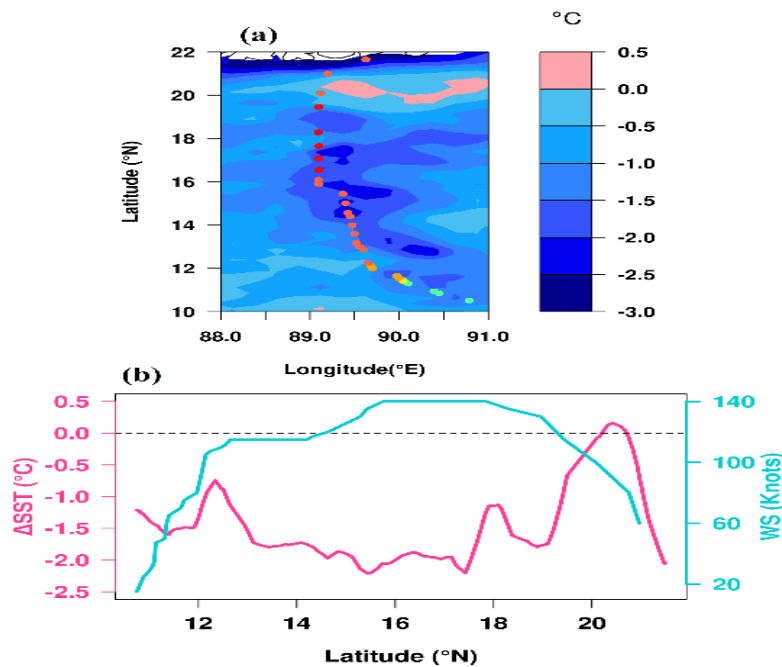


Figure 3:(a) SST anomaly (ECMWF Copernicus), taken as the difference between pre-cyclone and post-cyclone SSTs. Cyclone track is shown as filled solid circles with colour shades ranging from light green(category-1) to dark red (category-5). (b) SST anomaly (Pink solid line) and wind speed (blue solid line) along the cyclone track.

The cyclone-induced SST change is presented as SST anomaly (Figure 3a) between pre-cyclone (10 November 2007) and post-cyclone (16 November 2007). The observed SST anomaly shows the typical trend of the cyclone passage of the northern hemisphere, i.e., cooling to the right side of the track till 20°N, with a maximum value of 1.5°C. Followed by this cooling, a warm region is observed from 20°N - 22°N, with maximum warming to the range of < 0.5°C (Figure 3a). Sidr attains category-5 on 14 November 2007, when it crosses 20°N, where the SLTI gradient is significant as 3-4 °C (Thadathil et al. 2002). The cooling of the surface with the increase of wind speed can be noticed below 19°N, and thereafter SST increases even at the windspeed of 60 knots (Figure 3b). Correlations between surface wind speed and SST are always negative (Shukla and Misra 1977), which suggests that the observed warming can be attributed to the tapped heat from the SLTI by entrainment caused by the passage of Sidr.

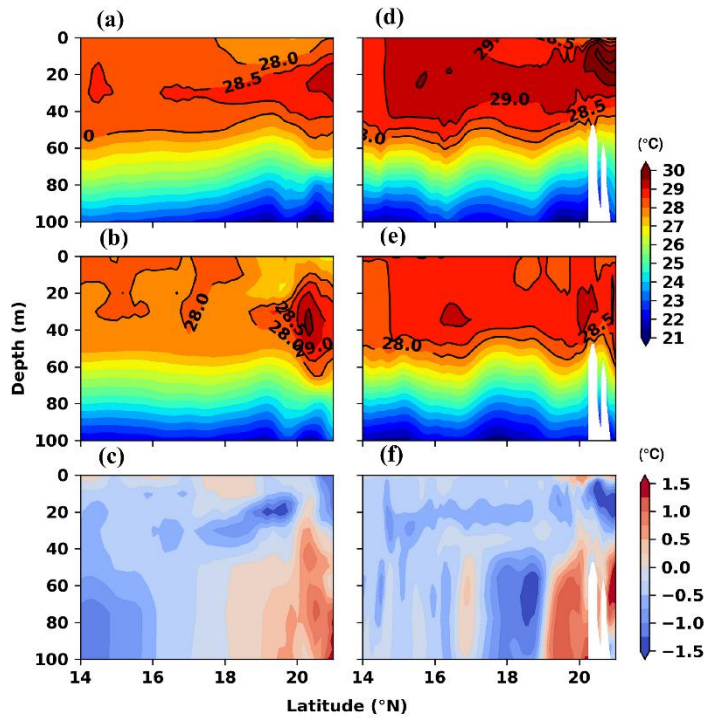


Figure 4: Temperature sections along 89.5°E from POM on (a) 10 November 2007 (Pre-cyclone); (b) 16 November 2007 (post-cyclone); (c) Temperature difference section plot (between (a) and (b)); Figures (d) to (f) represents similar plots with GLORYS model output.

This issue is addressed by analysing pre-cyclone and post-cyclone temperature sections taken from two models, namely POM and GLORYS. Figure 4a shows the longitudinal (89.5°E) pre-cyclone (10 November 2022) temperature section, matching the track of Sidr. Similarly, Figure 4b shows the POM temperature section for post-cyclone (16 November 2022). The temperature anomaly from these two sections is presented in Figure 4c. Similar GLORYS model output figures are presented in Figures 4d, 4e, and 4f, respectively. Both POM and GLORYS capture well the pre-cyclone strong inversion near the head bay and also the post-cyclone entrainment caused by Sidr. Both POM and GLORYS capture the surface layer warming caused by entrainment.

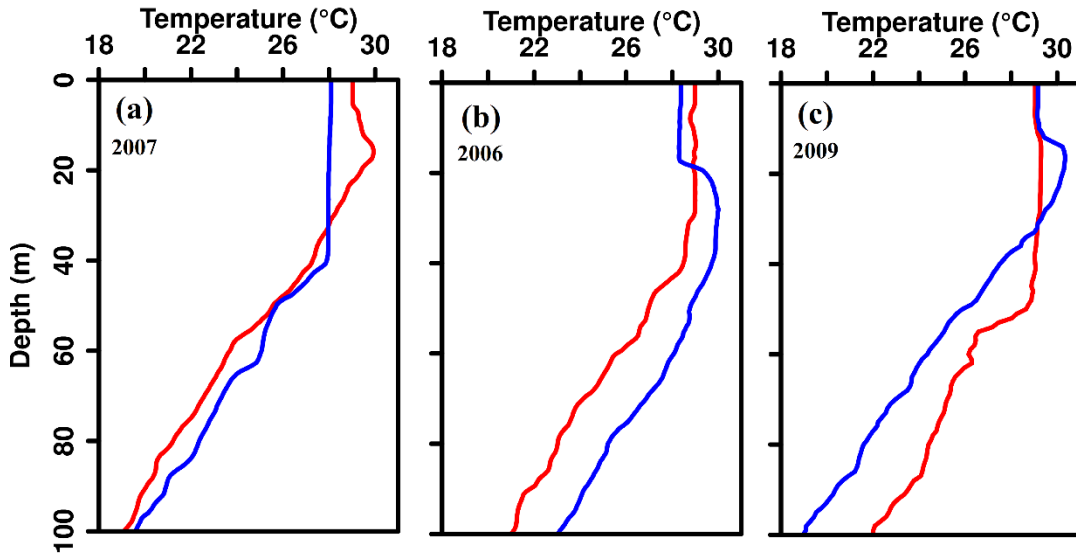


Figure 5: Temperature profiles from TOGA-XBT observations (Port Blair-Kolkata line) close to the cyclone track during October (red) and November (blue) in (a) 2007 (b) 2006 (c) 2009. Location of the observations is given in Figure-1.

In order to consolidate the model result of possible warming by entrainment of heat from the SLTI, we have examined the November 2007 XBT data from one station along the Port Blair-Kolkata TOGA-XBT line close to the cyclone track (marked as star in Figure-1a), where the SST warming is observed. Figure 5a illustrates temperature profiles up to 100 m at the location in the passage of Sidr (marked as star in Figure 1a). Temperature profiles for October and November 2007 are shown as red and blue lines, respectively. In the year 2007, a strong SLTI was visible during October (red), which vanished after the passage of Sidr in November (blue) (Figure 5a). In the case of non-cyclone years, SLTI during November is more organised and stronger, as depicted in Figures 5b and 5c. In November 2007, the temperature profile showed a near-mixed layer, indicating the cyclone-induced mixing and disappearance of SLTI. Figure 6a justifies the conclusion drawn on entrainment heating from POM and GLORYS, which results in the observed post-cyclone sea surface warming.

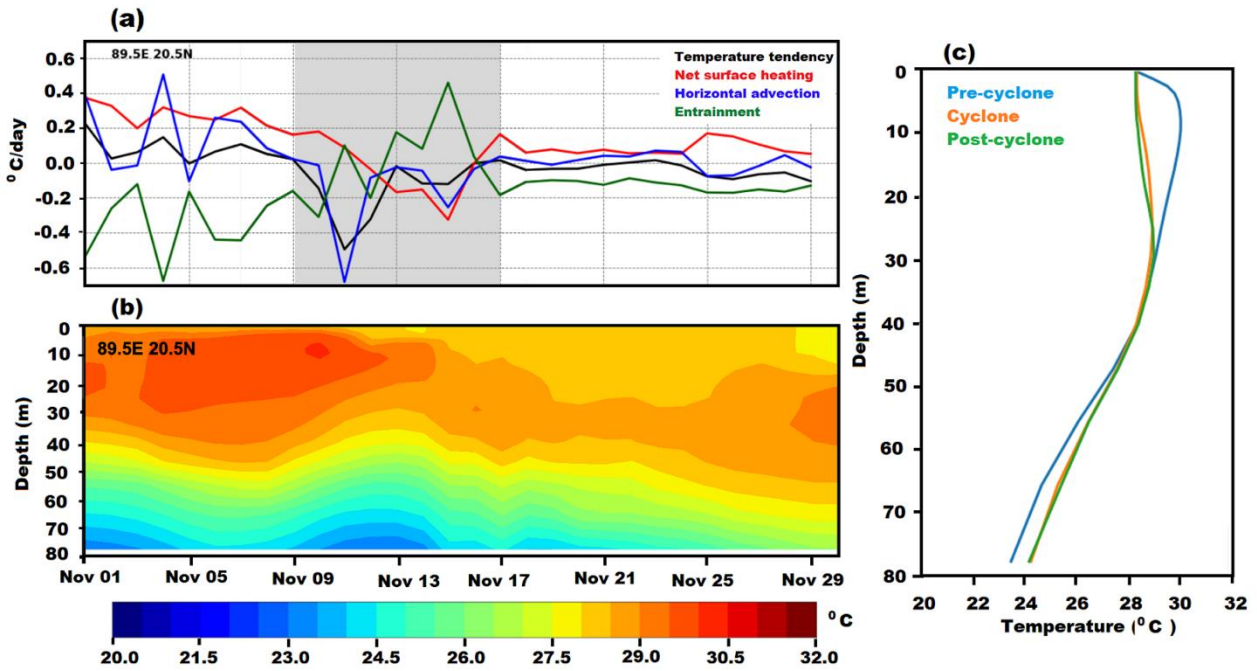


Figure 6: (a) Four components of the mixed layer heat budget; temperature tendency (black), net surface heat (red), horizontal advection (blue) and entrainment (green). Shaded region represents the study period (b) Temporal evolution of mixed layer temperature at the centre of the warming region (89.5°E , 20.5°N). (c) Vertical profile of temperature at the centre of the warming region during pre-cyclone (blue), cyclone (red) and post-cyclone (green).

Figure 6a shows the four components of the mixed layer heat budget; temperature tendency (black), net surface heat (red), horizontal advection through vertical advection and mixing (blue) and entrainment (green) at the location (89.5°E , 20.5°N) of the cyclone induced warming estimated from the GLORYS model output. Figure 6b shows the temporal evolution of surface layer temperature at the centre of the warming region (89.5°E , 20.5°N). Figure 6c shows the vertical profile of temperature at the centre of the warming region during pre-cyclone (blue), cyclone (red), and post-cyclone (green). The temperature tendency shows cooling prior to the arrival of the cyclone in the region. This can be attributed to the advection (green), which is very much evident from the simultaneous drop of values with that of temperature tendency. As the cyclone passes by, the entrainment supersedes the advection, and the temperature tendency starts to increase. All these reconfirm the role of entrainment in the near annihilation of the inversion layer and associated SST warming. This is well demonstrated in figure 6c, where the inversion layer (blue profile) is completely annihilated after the passage of the cyclone.

Discussion

SLTI distribution in the coastal water of BoB has certain characteristics in terms of its temperature

gradient. SLTI with larger temperature gradients is located near the coast compared to offshore (Thadathil et al. 2002). This distribution characteristic is attributed to the freshening effect of the water close to the coast from runoff. Therefore, when a cyclone approaches the coast, the possible entrainment of warmer water is likely to occur near the coast compared to offshore.

There are many studies on the effects of salinity-induced BL on TC development and intensification. BL promotes TC intensification [e.g., Wang et al. (2011), Neetu et al. (2012), Balaguru et al. (2012), Vissa et al. (2013), Domingues et al. (2015)]. However, it is also reported that the BL has a limited impact on TC intensification [Newinger and Toumi (2015), Hernandez, Jouanno, and Durand (2016)]. Yan, Li, and Wang (2017) reported that TC intensification due to the presence of BL is a complex process depending on the forcing time, stratification and intensity itself. The present study emphasises bringing out the effect of SLTI on SST warming. Without SLTI, the cyclone induces cooling that produces negative feedback on TC and its intensification. However, in the case of a surface layer with SLTI, the warm water can induce positive feedback on TC, leading to the intensification of the cyclone. Figure 3b shows the Sidr wind speed and the SST anomaly along its track. In spite of the warming, an intensification of the cyclone associated with possible positive feedback is not clearly seen here, which may be due to the immediate landfall of the cyclone after crossing the SLTI zone.

Cyclone Sidr attains category-1 in the central bay, where the BL is thin compared to that at the head bay. Therefore, cyclone-induced entrainment of cold water occurs in this region. This is visible in the SST anomaly (Figure 3a). As Sidr advances to the north, it attains category-5 near the head bay, where strong SLTI is present; the cyclone-induced mixing in this region brings warm water to the surface to cause the observed warming in this region. The mixing, deepening of the mixed layer and annihilation of the inversion layer are well exhibited in temperature profiles (Figure 5a). After the passage of the cyclone on 20 November, the vertical mixing was forced to annihilate the SLTI and distribute the temperature to form a deep mixed layer (Figure 5a). In the model results, the maximum temperature in the subsurface is noticed along 20°N (Figure 4a, 4d), which coincides with the surface warming noticed after the cyclone pass (Figure 3a). This scenario reinforces the conclusion drawn from the model results of POM and GLORYS on entrainment warming. As seen in Figure 6a, compared to other heating terms (temperature tendency, surface heating and horizontal advection), the entrainment term shows a positive tendency during the passage of cyclones of the location 89.5°E and 20.5°N . The presence of strong SLTI before the cyclone and weakening of SLTI during the passage of the cyclone due to entrainment and vertical mixing and a possible recurrence of SLTI after the passage of the cyclone is well depicted in Figure 6b. This is also well manifested in

Figure 6c. The tapped heating from the inversion layer significantly reduces cyclone-induced cooling and forces surface warming.

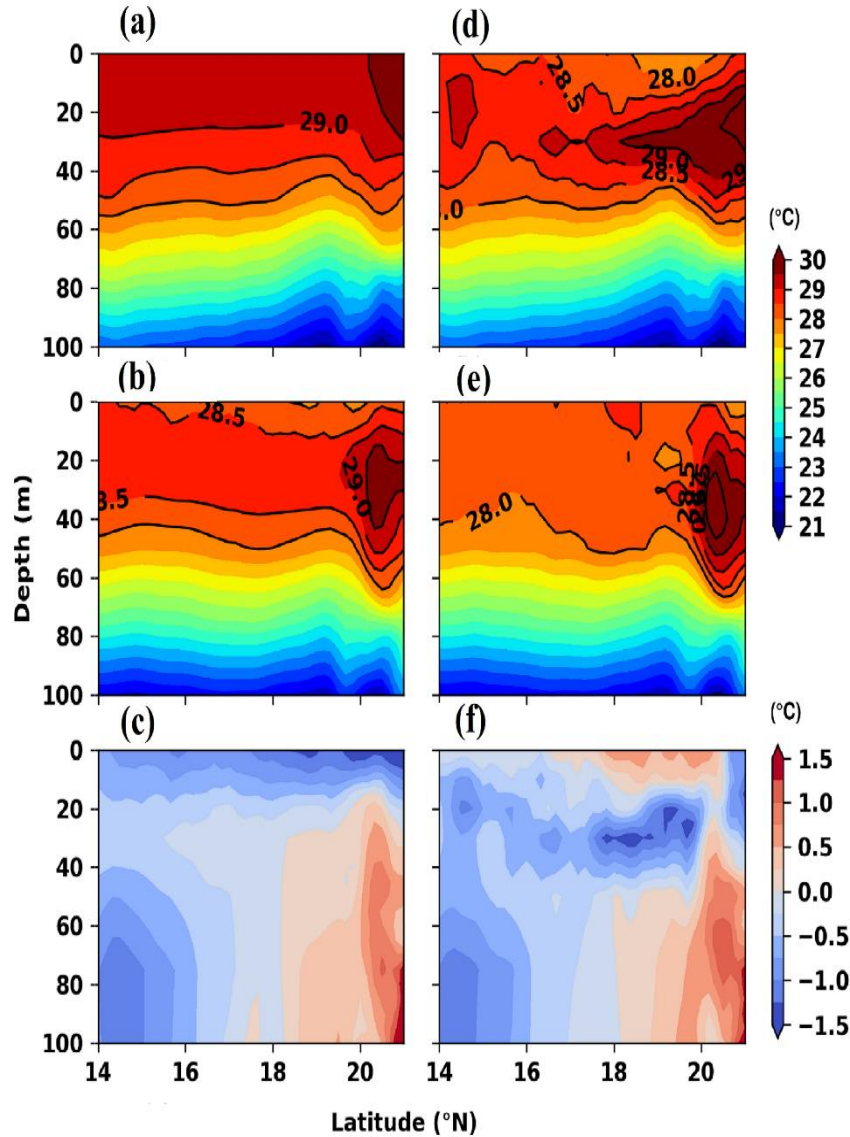


Figure 7: Temperature sections along 89.5°E from POM on Non-SLTI case (a) 10 November 2007 (Pre-cyclone) (b) 16 November 2007 (post-cyclone) (c) Temperature difference between (a) and (b). Figures (d) to (f) are the same but double the value of the actual SLTI gradient.

The 3-D POM model is further utilised to ascertain the role of SLTI-tapped heat in warming the surface layer. The model is run for different conditions viz. (a) non-inversion (b) double the value of the actual SLTI gradient, to study the sensitivity of inversion in the cyclone-induced SST changes (Fig. 7). In the case with no inversion, instead of warming the surface is cooled by $\sim 1.5^{\circ}\text{C}$. Whereas

in the case of higher SLTI (double the value of actual SLTI gradient), the surface layer warming is increased from normal case by around 0.7°C (0.5°C during normal to 1.2°C when SLTI gradient is double). Since category-5 cyclone passing through a high SLTI zone is limited, the model study and in-situ data are of prime importance. For a better understanding and appreciation of the process, a schematic shown in Figure 8 explains the role of each process involved in the observed warming. Thadathil et al. (2002; 2016) show that the SLTI in the BoB is subjected to strong intra-seasonal to inter-annual variability. The main candidate for the observed SLTI variability is the freshwater input through runoff and precipitation. This study also suggests the importance of incorporating the short-term variability of SLTI in cyclone forecasting models.

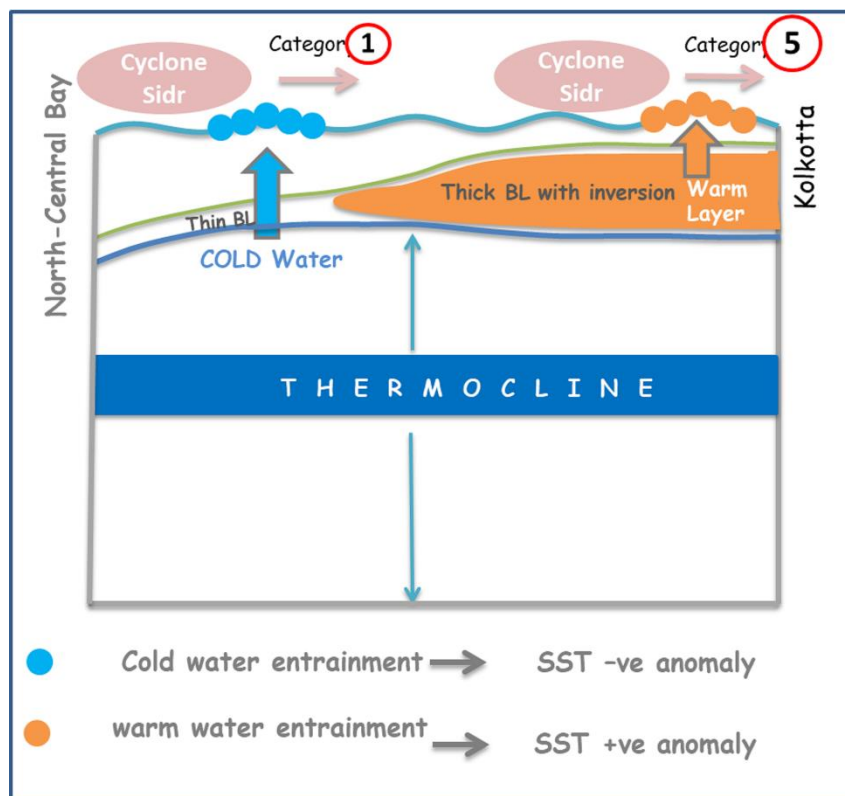


Figure 8: Schematic of the passage of Sidr with warm water entrainment from the inversion layer.

In the present study, we have addressed the role of Sidr, a category-5 cyclone. In order to establish the theory of post-cyclone SST warming due to SLTI, a composite analysis will be more appropriate instead of the case study from one cyclone (Sidr). The non-availability of data in this regard limited our study to Sidr. Although the case studies using the POM model strengthen the findings from the present study, analysis of observations from similar cyclones in future will reinforce the present findings.

Acknowledgements

The authors would like to acknowledge the encouragement and support from Director, Naval Physical and Oceanographic Laboratory, Kochi.

Data Availability Statement.

The cyclone parameters were obtained from the International Best Track Archive for Climate Stewardship (IBTrACS; Knapp et al. (2010)) dataset (<https://www.ncdc.noaa.gov/ibtracs>). Temperature and salinity fields were obtained from the World Ocean Atlas 2018 (<https://www.ncei.noaa.gov/>). The wind, solar radiation, sea surface temperature, net heat flux data from ERA5 fifth-generation ECMWF reanalysis Hersbach et al. (2020), and sea-level data from Copernicus Marine Environment Monitoring Service (CMEMS) were downloaded from the climate data store-Copernicus (<https://cds.climate.copernicus.eu>). Figures were made using the RStudio 2021.09.1+372 "Ghost Orchid" Release for Ubuntu Bionic. Python 3.9.5 was also used for creating plots. TOGA XBT data have been obtained from the National Institute of Oceanography, Dona Paula, Goa, India (<https://www.nio.org/>). Temperature sections before and after the cyclone along the track were plotted using model output from Princeton Ocean Model (Blumberg and Mellor (1987), (<http://www.ccpo.odu.edu/POMWEB/>) and Global Ocean Reanalysis and Simulations Lellouche et al. (2018).

References

- Ali, Anwar. 1999. "Climate Change Impacts and Adaptation Assessment in Bangladesh." *Climate Research* 12 (2-3): 109–16.
- Balaguru, Karthik, Ping Chang, R Saravanan, L Ruby Leung, Zhao Xu, Mingkui Li, and Jen-Shan Hsieh. 2012. "Ocean Barrier Layers' Effect on Tropical Cyclone Intensification." *Proceedings of the National Academy of Sciences* 109 (36): 14343–7.
- Beal, LM, Jerome Vialard, MK Roxy, J Li, M Andres, H Annamalai, M Feng, W Han, R Hood, T Lee, and M Lengaigne. 2020. "A Road Map to Indoos-2: Better Observations of the Rapidly Warming Indian Ocean." *Bulletin of the American Meteorological Society* 101 (11): E1891–E1913.
- Blumberg, Alan F, and George L Mellor. 1987. "A Description of a Three-Dimensional Coastal Ocean Circulation Model." *Three-Dimensional Coastal Ocean Models* 4: 1–16.
- Chowdhury, KM Azam, Wensheng Jiang, Guimei Liu, Md Kawser Ahmed, and Shaila Akhter. 2022a. "Spatiotemporal variation and mechanisms of temperature inversion in the Bay of Bengal and the eastern equatorial Indian Ocean." *Acta Oceanologica Sinica* 41, no. 4: 23-39.
- Chowdhury, KM Azam, Wensheng Jiang, Changwei Bian, Guimei Liu, Md Kawser Ahmed, and Shaila Akhter. 2022b. "Contributions of shortwave radiation to the formation of temperature inversions in the Bay of Bengal and eastern equatorial Indian Ocean: A modeling approach." *Acta Oceanologica Sinica* 41, no. 9: 19-37.

- Dee, Dick P, S M^{††} Uppala, Adrian J Simmons, Paul Berrisford, Paul Poli, Shinya Kobayashi, U Andrae, MA Balmaseda, G Balsamo, DP Bauer, and P Bechtold. 2011. "The Era-Interim Reanalysis: Configuration and Performance of the Data Assimilation System." *Quarterly Journal of the Royal Meteorological Society* 137 (656): 553–97.
- Domingues, Ricardo, Gustavo Goni, Francis Bringas, Sang-Ki Lee, Hyun-Sook Kim, George Halliwell, Jili Dong, Julio Morell, and Luis Pomales. 2015. "Upper Ocean Response to Hurricane Gonzalo (2014): Salinity Effects Revealed by Targeted and Sustained Underwater Glider Observations." *Geophysical Research Letters* 42 (17): 7131–8.
- Garcia, HE, KW Weathers, CR Paver, I Smolyar, TP Boyer, MM Locarnini, MM Zweng, AV Mishonov, OK Baranova, and D Seidov. 2019. "World Ocean Atlas 2018, Volume 3: Dissolved Oxygen, Apparent Oxygen Utilization, and Dissolved Oxygen Saturation."
- Hernandez, Olga, Julien Jouanno, and Fabien Durand. 2016. "Do the Amazon and Orinoco Freshwater Plumes Really Matter for Hurricane-Induced Ocean Surface Cooling?" *Journal of Geophysical Research: Oceans* 121 (4): 2119–41.
- Hersbach H, B Bell, P Berrisford, S Hirahara, A Horányi, J Muñoz-Sabater, J Nicolas, C Peubey, R Radu, D Schepers, and Simmons, A. 2020. "The Era5 Global Reanalysis." *Quarterly Journal of the Royal Meteorological Society* 146 (730): 1999–2049.
- Jian, Li, Yang Lei, Shu Ye-Qiang, and Wang Dong-Xiao. 2012 "Temperature inversion in the Bay of Bengal prior to the summer monsoon onsets in 2010 and 2011." *Atmospheric and Oceanic Science Letters* 5, no. 4: 290-294.
- Jullien, Swen, Patrick Marchesiello, Christophe E Menkes, Jérôme Lefèvre, Nicolas C Jourdain, Guillaume Samson, and Matthieu Lengaigne. 2014. "Ocean Feedback to Tropical Cyclones: Climatology and Processes." *Climate Dynamics* 43 (9): 2831–54.
- Knapp, Kenneth R, Michael C Kruk, David H Levinson, Howard J Diamond, and Charles J Neumann. 2010. "The International Best Track Archive for Climate Stewardship (Ibtracs) Unifying Tropical Cyclone Data." *Bulletin of the American Meteorological Society* 91 (3): 363–76.
- Krishna, VV, VSN Murty, MSS Sarma, and JS Sastry. 1993. "Thermal Response of Upper Layers of Bay of Bengal to Forcing of a Severe Cyclonic Storm: A Case Study."
- Kumar, PV Hareesh, Madhu Joshi, KV Sanilkumar, AD Rao, P Anand, K Anil Kumar, and CVK Prasada Rao. 2009. "Growth and Decay of the Arabian Sea Mini Warm Pool During May 2000: Observations and Simulations." *Deep Sea Research Part I: Oceanographic Research Papers* 56 (4): 528–40.
- Lellouche, Jean-Michel, Olivier Le Galloudec, Eric Greiner, Gilles Garric, Charly Regnier, Marie Drevillon, and PY Le Traon. 2018. "The Copernicus Marine Environment Monitoring Service Global Ocean 1/12 Physical Reanalysis Glorys12v1: Description and Quality Assessment." In *EGU General Assembly Conference Abstracts*, 20:19806.
- Li, Zhi, Weidong Yu, Tim Li, VSN Murty, and Fredolin Tangang. 2013. "Bimodal Character of Cyclone Climatology in the Bay of Bengal Modulated by Monsoon Seasonal Cycle." *Journal of Climate* 26 (3): 1033–46.
- Longshore, David. 2008. *Encyclopedia of Hurricanes, Typhoons, and Cyclones*. Infobase Publishing.

- Mondal, M., A Biswas, S Haldar, S Mandal, S Bhattacharya, and S Paul. 2022. "Spatio-temporal behaviours of tropical cyclones over the Bay of Bengal Basin in last five decades". *Tropical Cyclone Research and Review*, 11(1), pp.1-15.
- Maneesha, K, VSN Murty, M Ravichandran, T Lee, Weidong Yu, and MJ McPhaden. 2012. "Upper Ocean Variability in the Bay of Bengal During the Tropical Cyclones Nargis and Laila." *Progress in Oceanography* 106: 49–61.
- Mathew, Simi, Usha Natesan, G Latha, R Venkatesan, Rokkam R Rao, and M Ravichandran. 2018. "Observed Warming of Sea Surface Temperature in Response to Tropical Cyclone Thane in the Bay of Bengal." *Current Science*, 1407–13.
- Nadimpalli, Raghu, Shyama Mohanty, Nishant Pathak, Krishna K. Osuri, UC Mohanty, and Somoshree Chatterjee. 2021. "Understanding the characteristics of rapid intensity changes of Tropical Cyclones over North Indian Ocean." *SN Applied Sciences* 3: 1-12.
- Navaneeth, KN, MV Martin, K Jossia Joseph, and R Venkatesan. 2019. "Contrasting the Upper Ocean Response to Two Intense Cyclones in the Bay of Bengal." *Deep Sea Research Part I: Oceanographic Research Papers* 147: 65–78.
- Neetu, Suresh, Matthieu Lengaigne, Emmanuel M Vincent, Jerome Vialard, Gurvan Madec, Guillaume Samson, MR Ramesh Kumar, and Fabien Durand. 2012. "Influence of Upper-Ocean Stratification on Tropical Cyclone-Induced Surface Cooling in the Bay of Bengal." *Journal of Geophysical Research: Oceans* 117 (C12).
- Newinger, Christina, and Ralf Toumi. 2015. "Potential Impact of the Colored a Mazon and O Rinoco Plume on Tropical Cyclone Intensity." *Journal of Geophysical Research: Oceans* 120 (2): 1296–1317.
- Pothapakula, Praveen Kumar, Krishna K Osuri, Sujata Pattanayak, UC Mohanty, Sourav Sil, and Raghu Nadimpalli. 2017. "Observational Perspective of Sst Changes During Life Cycle of Tropical Cyclones over Bay of Bengal." *Natural Hazards* 88 (3): 1769–87.
- Rao, AD, Madhu Joshi, and M Ravichandran. 2008. "Oceanic Upwelling and Downwelling Processes in Waters Off the West Coast of India." *Ocean Dynamics* 58 (3): 213–26.
- Rao, RR, and R Sivakumar. 2000. "Seasonal Variability of Near-Surface Thermal Structure and Heat Budget of the Mixed Layer of the Tropical Indian Ocean from a New Global Ocean Temperature Climatology." *Journal of Geophysical Research: Oceans* 105 (C1): 995–1015.
- Sengupta, Debasis, Bharath Raj Goddalahundi, and DS Anitha. 2008. "Cyclone-Induced Mixing Does Not Cool Sst in the Post-Monsoon North Bay of Bengal." *Atmospheric Science Letters* 9 (1): 1–6.
- Shukla, J, and BM Misra. 1977. "Relationships between sea surface temperature and wind speed over the central Arabian Sea, and monsoon rainfall over India." *Monthly Weather Review*, 105(8), pp.998-1002.
- Sindhu, B, I Suresh, AS Unnikrishnan, NV Bhatkar, S Neetu, and GS Michael. 2007. "Improved Bathymetric Datasets for the Shallow Water Regions in the Indian Ocean." *Journal of Earth System Science* 116 (3): 261–74.

Sprintall, Janet, and Matthias Tomczak. 1992. "Evidence of the Barrier Layer in the Surface Layer of the Tropics." *Journal of Geophysical Research: Oceans* 97 (C5): 7305–16.

Subrahmanyam, Bulusu, VSN Murty, Ryan Sharp, James O'Brien, and others. 2005. "Air-Sea Coupling During the Tropical Cyclones in the Indian Ocean: A Case Study Using Satellite Observations." *Pure and Applied Geophysics* 162 (8): 1643–72.

Thadathil, Pankajakshan, VV Gopalakrishna, PM Muraleedharan, GV Reddy, Nilesh Araligidad, and Shrikant Shenoy. 2002. "Surface Layer Temperature Inversion in the Bay of Bengal." *Deep Sea Research Part I: Oceanographic Research Papers* 49 (10): 1801–18.

Thadathil, Pankajakshan, PM Muraleedharan, RR Rao, YK Somayajulu, GV Reddy, and C Revichandran. 2007. "Observed Seasonal Variability of Barrier Layer in the Bay of Bengal." *Journal of Geophysical Research: Oceans* 112 (C2).

Thadathil, Pankajakshan, Iyyappan Suresh, S Gautham, S Prasanna Kumar, Matthieu Lengaigne, RR Rao, S Neetu, and Akshay Hegde. 2016. "Surface Layer Temperature Inversion in the Bay of Bengal: Main Characteristics and Related Mechanisms." *Journal of Geophysical Research: Oceans* 121 (8): 5682–96.

Verezemskaya, Polina, Bernard Barnier, Sergey K Gulev, Sergey Gladyshev, Jean-Marc Molines, Vsevolod Gladyshev, Jean-Michel Lellouche, and Alexander Gavrikov. 2021. "Assessing Eddy (1/12°) Ocean Reanalysis Glorys12 Using the 14-Yr Instrumental Record from 59.5°N Section in the Atlantic." *Journal of Geophysical Research: Oceans* 126 (6): e2020JC016317.

Vinayachandran, PN, VSN Murty, and V Ramesh Babu. 2002. "Observations of Barrier Layer Formation in the Bay of Bengal During Summer Monsoon." *Journal of Geophysical Research: Oceans* 107 (C12): SRF–19.

Vissa, Naresh Krishna, ANV Satyanarayana, and B Prasad Kumar. 2013. "Response of Upper Ocean and Impact of Barrier Layer on Sidr Cyclone Induced Sea Surface Cooling." *Ocean Science Journal* 48 (3): 279–88.

Wang, XiDong, GuiJun Han, YiQuan Qi, and Wei Li. 2011. "Impact of Barrier Layer on Typhoon-Induced Sea Surface Cooling." *Dynamics of Atmospheres and Oceans* 52 (3): 367–85.

Webster PJ, Bradley EF, Fairall CW, Godfrey JS, Hacker P, Houze Jr RA, Lukas R,.

Webster, PJ, Edward F Bradley, CW Fairall, JS Godfrey, P Hacker, RA Houze Jr, R Lukas, Y Serra, JM Hummon, TD Lawrence, and CA Russell. 2002. "The Jasmine Pilot Study." *Bulletin of the American Meteorological Society* 83 (11): 1603–30.

Yan, Youfang, Li Li, and Chunzai Wang. 2017. "The Effects of Oceanic Barrier Layer on the Upper Ocean Response to Tropical Cyclones." *Journal of Geophysical Research: Oceans* 122 (6): 4829–44.